International Journal of Research in Engineering and Science (IJRES)
ISSN (Online): 2320-9364, ISSN (Print): 2320-9356
www.ijres.org Volume 13 Issue 5 ǁ May 2025 ǁ PP. 247-254

Expression Characteristics of BmIDH and Its Effects on Microsporidian Proliferation

Nan Hu [1,2,*], Yi Liu [1,2], Tingting Yu [1,2] and Qi Tan [1]

[1] *College of Chemical Engineering, Sichuan University of Science & Engineering, Zigong 643002, China*
[2] *Institute of Precision Medicine, Zigong Academy of Big Data and Artificial Intelligence in Medical Science, Zigong Fourth People's Hospital, Zigong 643000, China*
* *Correspondence: susehn@163.com*

Abstract: *Microsporidia like Nosema bombycis cause severe sericulture losses. This study investigates Bombyx mori isocitrate dehydrogenase (BmIDH), a TCA cycle enzyme, in host-energy metabolism during infection. Transcriptome and qPCR show 10–140-fold BmIDH upregulation post-N. bombycis infection. Immunolocalization reveals cytoplasmic and mitochondrial BmIDH localization. Overexpression enhances cellular ATP production, glucose uptake, and proliferation, accelerating N. bombycis growth by boosting host energy metabolism. Inhibition of glucose uptake with BAY-876 reduces ATP and suppresses microsporidian proliferation, even in BmIDH-overexpressing cells. BmIDH promotes infection via TCA cycle acceleration, serving as a potential anti-parasitic target. Glucose uptake blockade via BAY-876 represents a promising strategy against microsporidia.*

Keywords: *Microsporidia; Nosema bombycis; BmIDH; Energy metabolism*

Date of Submission: 20-05-2025 Date of acceptance: 31-05-2025

I. INTRODUCTION

Microsporidia are typical single-celled microorganisms [1]. Most of their parasitic processes occur inside host cells, and they are a group of pathogens with the characteristics of both eukaryotes and unicellular organisms [2-5]. Widely distributed in nature, Microsporidia often cause significant economic losses to farmed animals such as silkworms, bees, and fish [6,7]. As independent cellular organisms, Microsporidia spend important parts of their life cycle in a parasitic state, relying on absorbing substances and energy from host organisms to compensate for their own metabolic deficiencies. Nosema bombycis, a representative species of the Nosema genus, has become a statutory quarantine object for silkworm seed testing in China due to its dual transmission modes (horizontal and vertical), both of which can cause severe economic damage to sericulture upon infection. The intracellular parasitic characteristics of Microsporidia indicate extensive material and energy exchange with their hosts. Lacking complete metabolic pathways and limited energy synthesis capabilities, these parasites are highly dependent on host-derived energy for proliferation. Studying how Microsporidia compete with hosts to obtain energy and materials is crucial for clarifying parasitic invasion and pathogenic mechanisms, and it provides important reference values and guiding significance for the prevention and control of parasitic pathogens and the development of anti-infective drugs.

The genome of N. bombycis has undergone evolutionary reduction, retaining only core material synthesis and metabolic pathways while lacking a complete pyruvate dehydrogenase complex and tricarboxylic acid (TCA) cycle pathway [8]. Research on the regulation of host energy metabolism by N. bombycis can enhance our understanding of the interaction between the pathogen and the host during infection, which is of great significance for deciphering the molecular mechanisms of N. bombycis parasitism. Additionally, it provides data support and theoretical basis for screening molecular targets of anti-Microsporidia drugs. Based on this, carrying out molecular breeding research to create silkworm strains resistant to pebrine is a research work of significant importance and value.

Outside host cells, Microsporidia exist in a dormant state resistant to environmental stresses. Some species can survive for years under appropriate conditions while maintaining infectivity [9]. Meanwhile, Microsporidia infection is a rapid ATP-dependent biological process; for example, the unwinding and ejection of polar tubes require ATP [10,11]. Therefore, dormant spores must synthesize their own energy. On the other hand, organisms living within another cell face altered selective pressures. Surrounded by host metabolites (e.g., nucleotides and amino acids), Microsporidia can more easily acquire metabolic compounds, thereby reducing endogenous metabolite production.

In multiple reported Microsporidia species, the genome lacks genes encoding PDH E2 and E3 subunits. These genes function similarly to bacterial diphosphate-dependent thiaminases, catalyzing the oxidative

decarboxylation of pyruvate to produce acetate and carbon dioxide [12-17]. Acetate can be converted into acetyl-CoA via acetyl-CoA synthetase. Due to the absence of TCA cycle and fatty acid synthase complexes in Microsporidia, acetyl-CoA may serve as a substrate for forming dimethylallyl pyrophosphate and isopentenyl pyrophosphate in the mevalonate pathway, which are intermediates in important pathways such as protein acetylation and steroidogenesis. Genome reduction in Microsporidia limits their own material synthesis, making them dependent on host-derived substances. During infection, regulating host energy metabolism to promote ATP production is a strategy beneficial for Microsporidia proliferation.

Energy metabolism is the foundation for maintaining life activities and internal environmental homeostasis. Glucose is the most direct energy source for cells. In normal cells, glucose is typically converted into ATP through glycolysis, the TCA cycle, and oxidative phosphorylation [18]. After entering cells, glucose is first catalyzed by hexokinase (HK) to form glucose-6-phosphate, followed by reactions catalyzed by enzymes such as phosphofructokinase (PFK) and pyruvate kinase (PK), which release energy and produce pyruvate [19]. Under hypoxic conditions, pyruvate is converted into lactate; under aerobic conditions, it is catalyzed by pyruvate dehydrogenase (PDH) to form acetyl-CoA. Acetyl-CoA combines with oxaloacetate to form citrate, which enters the TCA cycle for oxidative energy production. Citrate is converted into isocitrate (ICT) by aconitase, and isocitrate dehydrogenase (IDH) catalyzes the first dehydrogenation step. The energy required for the spore stage of Microsporidia is typically provided by trehalose metabolism and glycolysis, and Microsporidia genomes contain all genes encoding glycolytic enzymes. The presence of glycerophosphate shuttles in mitochondrial and cytoplasmic components indicates that electrons generated during glycolysis can be transported to the degenerated mitochondrial organelle, the mitosome.

IDH is an enzyme family widely distributed in organisms, catalyzing the oxidative decarboxylation of isocitrate to α-ketoglutaric acid (α-KG) using NADP or NAD as coenzymes. This reaction catalyzed by IDH is not only an essential step in the TCA cycle but also an important source of intracellular NADPH/NADH, playing a key role in maintaining cellular redox balance [20]. In eukaryotes, IDH exists in two forms: NADP-dependent and NAD-dependent. NADP-dependent IDH is widely present in mitochondria, cytoplasm, and peroxisomes, contributing to cellular anti-oxidative damage, detoxification of reactive oxygen species, and synthesis of fats and cholesterol. NAD-dependent IDH primarily resides in mitochondria and acts as a rate-limiting enzyme in the TCA cycle. In mammals, NAD-dependent IDH is allosterically regulated by TCA cycle metabolites (e.g., citrate and ADP), which alter its affinity for isocitrate with minimal impact on maximum reaction rate. IDH mutations are implicated in oncogenesis; mutations in IDH1 and IDH2 have been identified in human tumors such as gliomas, chondrosarcomas, and cholangiocarcinomas. In tumor cells, IDH mutations lead to loss of normal function and conversion of α-KG to the oncometabolite 2-hydroxyglutaric acid (2HG), which accumulates in mutated tumor cells and causes DNA or histone hypermethylation. Under normal cellular conditions, IDH functions are critical for intracellular glucose metabolism and homeostasis. However, our preliminary studies showed that BmIDH (Bombyx mori IDH) is upregulated upon N. bombycis infection. Whether BmIDH shares functional characteristics with mammalian IDH, its role in N. bombycis infection, and whether its function in cellular energy metabolism changes require further clarification.

In recent years, studies on Microsporidia-host interactions have revealed that infection can affect host cell cycle progression and apoptosis pathways [7,21,22], with energy metabolism regulation being a key component of pathogen-host interactions. Microsporidia infection typically induces drastic changes in host physiological and biochemical metabolism, forming a complex interaction network between the pathogen and the host [23]. Due to their inefficient energy metabolism, effective utilization of host ATP is critical for intracellular parasitism. This involves two aspects: first, enhancing host energy metabolism to produce more metabolites and ATP (with the core metabolic pathway, the TCA cycle, playing a major role); second, efficiently transporting host-generated ATP into the sporoplasm [24].

Our preliminary transcriptome analysis showed that the TCA cycle rate-limiting enzyme, B. mori isocitrate dehydrogenase, was induced to upregulate by 10-25 fold at multiple time points after N. bombycis infection. Quantitative validation revealed that IDH expression in infected cells was up to 20-140 fold higher than in control cells, suggesting its critical role in N. bombycis infection.

To better understand the energy metabolism interaction pattern between N. bombycis and its host and decipher the core mechanisms of intracellular parasitism, further research was conducted to investigate how Microsporidia hijack and regulate host energy metabolic pathways, induce and utilize host energy metabolism, and modulate the entire energy metabolic network during infection.

II. MATERIALS AND METHODS

2.1 ATP Content Assay

Sample Preparation： Samples were collected as previously described, lysed with 200 μL lysis buffer at 4°C or on ice bath. The lysed samples were centrifuged using a cold centrifuge at 4°C, 12,000 g for 5 min. The supernatant was collected for subsequent use. Standard Curve Preparation： The ATP standard was first diluted

with ATP assay lysis buffer on ice bath to prepare three concentration gradients: 0.1, 1, and 10 μmol/L. Preparation of ATP Assay Working Solution： 100 μL of ATP assay working solution was added to each sample. The working solution was diluted with lysis buffer at a ratio of 1:100 and kept on ice bath until use. ATP Concentration Measurement： Add 100 μL of ATP assay working solution to each sample, and let stand for 3–5 min to eliminate the background signal from the ATP baseline level. Transfer 20 μL of the sample to a microplate, mix immediately, and measure using a microplate reader. Calculate the ATP concentration in samples based on the standard curve.

2.2 Isolation and Purification of Tissue RNA

This experiment used the Total RNA Kit II (OMEGA), with detailed procedures following the manufacturer's instructions. Silkworm larvae infected with purified microsporidiawere sampled at 12, 24, 36, 48, 60, 72, and 120 h post-infection to extract RNA from midgut tissues. For each time point, ten infected larvae were randomly selected and pooled as one sample. Tissues were briefly washed with 1× PBS, quickly transferred to centrifuge tubes, and stored in liquid nitrogen until all time points were collected for unified grinding and RNA extraction. Samples were thoroughly ground into powder in liquid nitrogen, transferred to RNase-free centrifuge tubes, and rapidly mixed with 1 mL Trizol reagent or RNA-Solv® Reagent for lysis. The lysed samples were centrifuged at 4°C, 12,000 g for 15 min. The supernatant was transferred to a new tube containing 200 μL pre-cooled chloroform, mixed, and placed on ice bath for 10 min. The samples were centrifuged again under the same conditions. The upper aqueous phase was transferred to a new tube, and approximately 1/2 volume of absolute ethanol was added. The mixture was inverted 15–20 times to mix thoroughly. The mixture was transferred to an RNA adsorption column, allowed to stand for 10 min, and centrifuged at 10,000 g for 2 min. The waste liquid was discarded, and 400 μL RNA Wash Buffer I was added to the column. After standing at room temperature for 5 min, the column was centrifuged at 10,000 g for 1 min. The waste was discarded, and 300 μL RNA Wash Buffer I was added, followed by centrifugation at 10,000 g for 1 min. The waste was discarded, and 500 μL RNA Wash Buffer II was added. After standing for 3 min, the column was centrifuged at 10,000 g for 1 min. After discarding the waste, the column was centrifuged at 10,000 g for 3 min to remove residual wash buffer. The adsorption column was transferred to a 1.5 mL RNase-free centrifuge tube, and 30–50 μL DEPC water was added. After standing at room temperature for 5 min, RNA was eluted by centrifugation at 10,000 g for 3 min. The eluted RNA was kept on ice, and a small aliquot was used for concentration measurement. The remaining RNA was stored at -80°C.

2.3 Reverse Transcription of RNA

Part of the extracted RNA was used for reverse transcription to synthesize cDNA for subsequent experiments.Prior to reverse transcription, DNA was digested with DNase. The reaction system included: 2.0 μL 5×gDNA Eraser Buffer, 1.0 μL gDNA Eraser, 1.0 μg Total RNA (calculated based on concentration), and RNase-Free ddH2O to make up to 10 μL.The reaction mixture was incubated at 42°C for 2 min, then rapidly cooled to 4°C.The treated solution was mixed with the following components: Reaction solution from Step 1 in10.0 μL; 5×PrimeScript Buffer 2 (for Real Time) in 4.0 μL; RT Primer Mix in 1.0 μL; PrimeScript RT Enzyme Mix I in 1.0 μL; RNase-Free dH2O 4.0 μL. The mixture was subjected to reverse transcription in a PCR machine with the following program: 37°C for 30 min; 85°C for 5 s; hold at 4°C. The cDNA product was stored at -20°C.

2.4 Quantitative Real-Time PCR (qRT-PCR)

The prepared reaction mix was added to a 96-well plate with three technical replicates per sample. After centrifugation, the plate was placed in a qPCR machine with the following program: 95°C for 30 s; 40 cycles of 95°C for 5 s and 60°C for 15 s; followed by a melting curve analysis from 65°C to 95°C at 0.5°C increments every 5 s.

2.5 Immunofluorescence Assay

Immunofluorescence detection was performed on transfected cells as follows:

Cells were gently rinsed twice with 1×PBS for 3–5 min each. 400 μL of 4% paraformaldehyde (pre-cooled at 4°C) was added to each well, and cells were fixed at room temperature for 15 min. Paraformaldehyde was removed, and cells were washed five times with PBST (PBS containing 0.2% Tween20) for 6 min each. 400 μL of 0.1% Triton X-100 was added for permeabilization, and cells were incubated at room temperature for 10 min. Triton X-100 was removed, and cells were washed five times with 1×PBST for 6 min each. Cells were blocked with 1×PBS containing 10% sheep serum and 1% BSA at 37°C for 2 h. Primary antibody diluted 1:200 in blocking buffer was added to 24-well plates, and cells were incubated at 37°C for 1 h. Blocking buffer was removed, and cells were washed five times with 1×PBST for 6 min each. Fluorescently labeled secondary antibody diluted in blocking buffer was added, and cells were incubated at 37°C for 1 h. Nuclei were stained with DAPI at room temperature for 10 min. Cells were washed five times with PBST for 6 min each. Coverslips were mounted on slides with nail polish and observed under a confocal microscope.

2.6 Extraction of Cellular Genomic DNA

Cells infected with microsporidia or transfected with plasmids were gently resuspended by pipetting, transferred to 1.5 mL centrifuge tubes, and centrifuged at 1,000 g for 10 min at 4°C. The supernatant was discarded, and cells were washed with 1×PBS, resuspended, and centrifuged again under the same conditions. 300 μL DNAzol was added, and the mixture was vortexed for 15 s to lyse cells. The lysate was centrifuged at 10,000 g for 10 min at 4°C. Pre-cooled ice-cold ethanol was prepared. The supernatant was transferred to 1/2 volume of ice-cold absolute ethanol, mixed gently by inversion until white flocculent DNA appeared, and centrifuged at 50,000 g for 5 min at 4°C. Most of the supernatant was carefully discarded, and residual supernatant was removed with a pipette to avoid losing DNA. 800 μL of 75% ethanol was added for washing, followed by centrifugation at 5,000 g for 5 min at 4°C. This wash step was repeated once. Ethanol was carefully removed with a pipette, and the tube was left open to air-dry residual ethanol for 10–15 min. 50 μL of ultrapure water was added, and DNA was dissolved at 60°C for 2 h. 1 μL was used for concentration measurement, and the rest was stored at -20°C.

2.7 Glucose Content Assay

Cell culture supernatants from plasmid-transfected cells were collected and centrifuged at 1,000 g for 5 min. The supernatant was assayed by adding working solution at a sample:working solution ratio of 1:100, with three replicates per group. Samples were incubated at 37°C for 15 min, and absorbance at 505 nm was measured using a microplate reader. Glucose consumption in the medium was calculated using the formula: Glucose concentration (mmol/L) = [(Sample OD - Blank OD) / (Calibrator OD - Blank OD)] × Calibrator concentration.

2.8 Cell Proliferation and Viability Assay

Transfected cell suspensions were seeded into 96-well plates at 100 μL per well. 20 μL of CellTiter 96 AQueous One Solution Reagent was added to each well, and plates were incubated for 4 h. Absorbance at 490 nm was measured at 1 h, 2 h, and 4 h using a microplate reader.

III. RESULT

3.1 Sequence and Structural Analysis of BmIDH

The clustering of host energy metabolism-related differential pathways indicated a pronounced response in the tricarboxylic acid (TCA) cycle pathway, which is beneficial for stimulating the host to produce more ATP. Among these, Bm2860_46 showed the most significant upregulation fold. Quantitative PCR (qPCR) verification of Bm2860_46 expression after microsporidian infection revealed a substantial upregulation of Bm2860_46 transcription (Fig. 1), suggesting that Bm2860_46 plays a critical role in the intracellular parasitic process and may be hijacked by microsporidia.

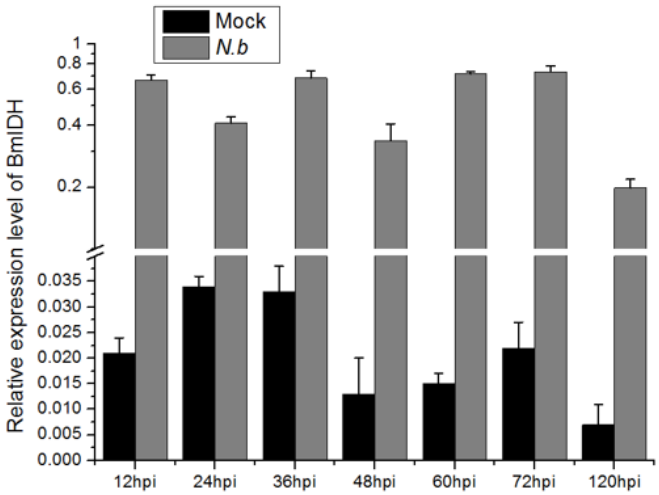

Fig. 1 Relative expression levels of Bm2860_46 detected by quantitative PCR after microsporidian infection. Mock: negative control.N.b: Group infected with N.bombycis. The abscissa represent the infection time point, and the ordinate represent the relative expression level of Bm2860_46.

Gene annotation identified Bm2860_46 as a member of the isocitrate dehydrogenase (IDH) family, named BmIDH in this study. Bioinformatics analysis of the BmIDH gene sequence showed that the full-length mRNA sequence is 1,227 bp, encoding 408 amino acids. Software prediction indicated that the molecular weight of the BmIDH protein is 46.17 KDa, with an isoelectric point of 6.67. Online prediction via the Smart website showed that the 8–398 amino acid sequence region of the BmIDH protein constitutes its conserved isocitrate

dehydrogenase functional domain (Fig. 2).

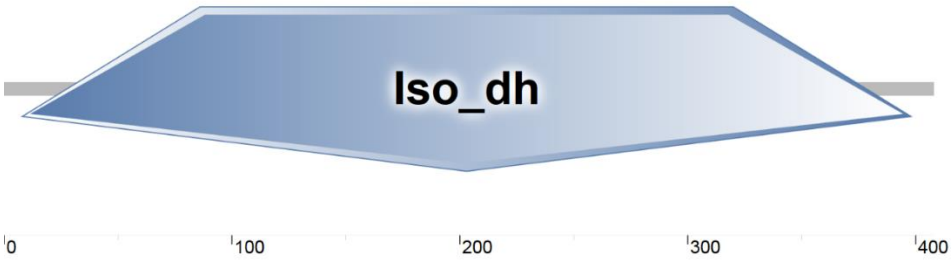

Fig. 2 Conserved functional domain of BmIDH

3.2 Cloning and Subcellular Localization of the BmIDH Gene

To investigate the function of BmIDH, a eukaryotic expression vector for BmIDH was constructed. Forty-eight hours after transfecting the plasmid into *Bombyx mori* BmN-SWU1 cells, immunofluorescence was used to detect BmIDH localization. Anti-Flag was used as the primary antibody, and red-fluorescently labeled goat anti-rabbit secondary antibody was applied. The nucleus was stained with DAPI, and mitochondria were labeled with Mito-Tracker Green. Observations were made using a confocal microscope.

Results showed (Fig. 3) that pIZ-BmIDH-Flag successfully expressed the BmIDH protein. The overexpressed BmIDH protein was localized in the cytoplasm of *BmN-SWU1* cells and co-localized with mitochondria.

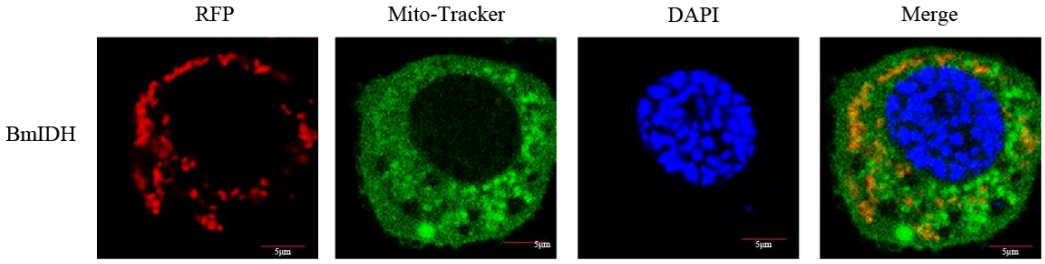

Fig. 3 Subcellular localization of BmIDH. RFP is the red fluorescence motivated by the label antibody, which represents the localization of the target protein. Mito-tracker stands for mitochondrial localization. DAPI is dye of nucleic acid; Merge: Merge diagram. Scale: 5 m.

3.3 Effects of BmIDH Overexpression on Cellular Energy Metabolism and Microsporidian Proliferation

As a rate-limiting enzyme in the TCA cycle, changes in BmIDH expression levels must influence cellular metabolism. Increased BmIDH expression is expected to promote the TCA cycle, thereby enhancing cellular ATP production.

Under conditions of sufficient glucose in the medium, cells transfected with the BmIDH expression plasmid were grouped by time points to detect intracellular ATP content, with the empty vector serving as the control. Results showed that BmIDH overexpression significantly enhanced host ATP production, with significant differences from the control group detected as early as 24 h post-transfection (h p.t.), and the promotion efficiency gradually plateaued over time (Fig. 4A).

To investigate whether the promotion of host ATP production by BmIDH occurs via enhanced glycolysis, glucose consumption in the culture medium was measured at multiple time points under the same conditions. Results showed (Fig. 4B) that cells overexpressing BmIDH absorbed significantly more glucose from the medium than control cells, with this significance detected at 24 h p.t. and exhibiting a time-dependent effect.

MTS assays were used to detect cell proliferation viability after BmIDH overexpression. Results showed (Fig. 4C) that enhanced MTS conversion was detected at 24 h p.t., and significant differences between the transfected group and the control group were observed at multiple subsequent time points, indicating that BmIDH promotes cellular metabolism.

Given that BmIDH enhances cellular metabolism and promotes ATP production, and that BmIDH was found to be highly upregulated during microsporidian infection, we hypothesized that microsporidia may promote BmIDH expression to better acquire host energy resources during intracellular parasitism. To validate this, microsporidian infection was performed on cells transfected with the BmIDH plasmid or empty vector, and RNA was collected at different time points post-infection to quantify NbSSU transcript levels via qPCR. Results showed (Fig. 4D) that NbSSU transcription was detected in both groups, but transcription was more rapid in the BmIDH-overexpressing group, indicating that BmIDH enhances microsporidian proliferation in cells.

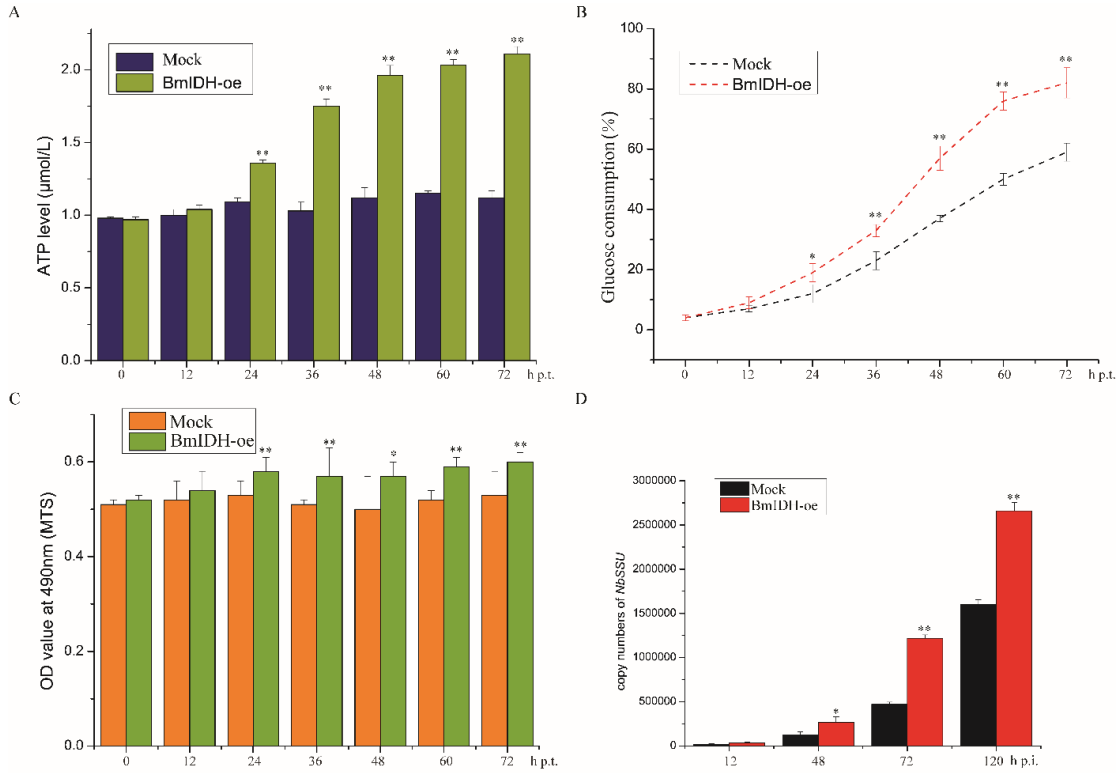

Fig. 4 Effects of BmIDH overexpression on cellular energy metabolism and microsporidian proliferation. (A) ATP level determination. (B) Glucose uptake rate measurement. (C) MTS metabolism detection. (D) The proliferation rate of *N.bombycis*. Mock: negative control. BmIDH-oe: *BmIDH* overexpression. N.b: *N.bombycis* infection. The abscissa represents the time point of infection Asterisks mean the difference was statistically significant (*: p <0.05, **: p <0.01).

3.4 Effects of Glucose Uptake Inhibition on Microsporidian Proliferation

Although BmIDH overexpression promotes cellular glucose uptake, BmIDH knockout does not significantly reduce glucose uptake. Given that reduced cellular ATP synthesis affects microsporidian proliferation, we investigated whether inhibiting GLUT1-mediated glucose transport could decrease ATP production and suppress microsporidian proliferation. Cells were treated with the GLUT1-specific inhibitor BAY-876 (0.005 μM), with DMSO as the control, and cellular ATP content was measured. Results showed (Fig. 5A) that ATP levels in inhibitor-treated cells were significantly lower than those in the control group. Overexpressing BmIDH in inhibitor-treated cells did not significantly increase ATP content, with only a marginal recovery observed at 72 h. These results indicate that BAY-876 effectively inhibits GLUT1-mediated glucose transport, reduces glycolytic activity, impairs energy metabolism, and decreases intracellular ATP content.

Microsporidian infection was performed on inhibitor-treated cells (with or without BmIDH overexpression), and NbSSU expression was analyzed. Results showed (Fig. 5B) that microsporidian proliferation was significantly suppressed in BAY-876-treated cells, suggesting that blocking cellular glucose uptake may be a potential strategy to inhibit microsporidian proliferation.

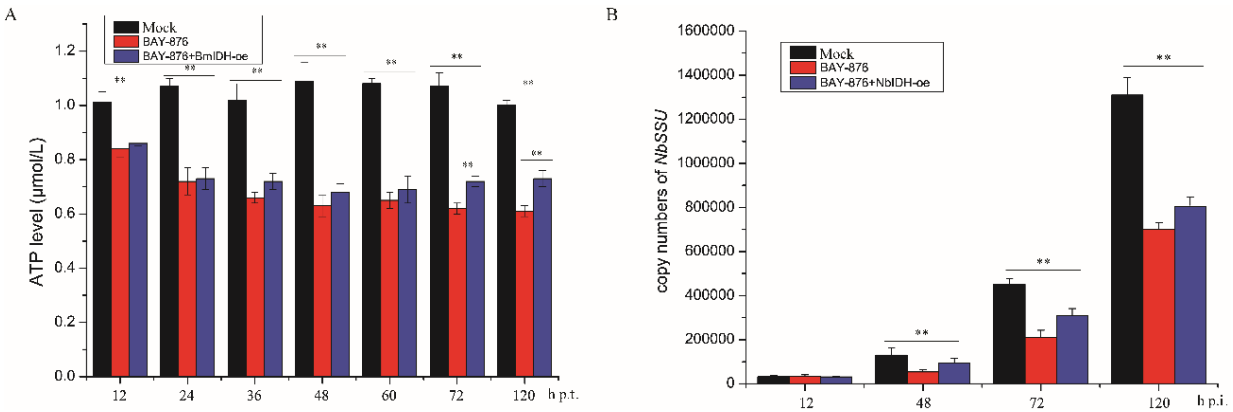

Fig. 5 Changes in cellular ATP content and microsporidian proliferation after BAY-876 treatment. (A) ATP detection after inhibitor treatment. (B) Detection of the proliferation rate of *N.bombycis*. Black column was treated with DMSO, red column was treated with 0.005 μM BAY-876 inhibitor, and blue column was treated by inhibitor with *BmIDH* overexpressed. Mock: negative control. BmIDH-oe: overexpression of *BmIDH*. The abscissa represents the time point of infection Asterisks mean the difference was statistically significant (*: $p < 0.05$, **: $p < 0.01$).

IV. DISCUSSION

The infection of microsporidia exerts multifaceted impacts on hosts. One aspect involves the evolution of regulatory mechanisms against host innate immune responses during long-term parasitism. For example, Nosema bombycis can secrete serine protease inhibitors (serpins) to modulate host melanization immunity or inhibit host apoptosis. The other aspect involves the induction and regulation of host energy metabolism. During the infection of hosts by Encephalitozoon cuniculi, a hexokinase with a signal peptide is secreted to participate in regulating host energy metabolism. In previous studies by our laboratory, the hexokinase NbHK of Nosema bombycis was identified and found to possess both a signal peptide and secretory activity, while enhancing the host's glycolytic pathway. Analyses in the previous research showed that Nosema bombycis affects multiple metabolic pathways in the host, indicating that its parasitic infection of silkworms is strategic. Among these host metabolic pathways, the gene encoding the rate-limiting enzyme of the tricarboxylic acid (TCA) cycle pathway showed the most significant upregulation at various infection time points, suggesting that this gene plays a critical role in the microsporidian infection process.

Bm2860_46 is an isocitrate dehydrogenase family gene named BmIDH. The BmIDH protein contains a conserved IDH domain and serves as the rate-limiting enzyme of the TCA cycle. When overexpressed, BmIDH localizes to the cytoplasm and exhibits colocalization with cellular mitochondria, providing a subcellular localization basis for its metabolic regulatory function. Infections by some microsporidian species lead to the enrichment or adsorption of host cell mitochondria, facilitating better utilization of mitochondria for substance and energy exchange. Similar phenomena have been observed in Nosema bombycis infections, indicating that host mitochondria, as the most critical energy metabolicorgans after infection, may participate in the interaction process of substance and energy exchange with microsporidia. The highly upregulated BmIDH is likely hijacked by microsporidia through some mechanism to promote cellular metabolism for the benefit of microsporidia.

The overexpression of BmIDH promotes microsporidian proliferation, which may benefit from BmIDH's ability to enhance cellular ATP synthesis. The transcriptional level of BmIDH is significantly upregulated after microsporidian infection, indicating that the activity of the BmIDH promoter is stimulated and activated by microsporidian infection. Two potential mechanisms for BmIDH transcriptional activation are hypothesized: First, upon invasion by pathogenic microorganisms, insects activate innate immune pathways to resist pathogens. After pathogen recognition, signal transduction mechanisms activate the intracellular transcriptional regulation system to generate corresponding responses. In silkworms, identified pathways such as the Toll signaling pathway and JAK/STAT pathway are involved in the confrontation with pathogens; Second, microsporidia may directly or indirectly regulate host cell transcription through secreted proteins. Although secretory transcription factors from Nosema bombycis have not been reported, the promotional effect of BmIDH on microsporidian proliferation suggests the possibility of active transcriptional regulation by the pathogen.

Furthermore, given the characteristic of highly induced transcriptional upregulation of BmIDH, screening its promoter and artificially optimizing it by removing basal promoter activity fragments while selecting fragments with high inductive activity may yield a microsporidian-inducible promoter. Such a promoter would have low basal transcriptional activity but could rapidly respond to microsporidian infection to induce target gene expression, making it a powerful tool for genetic engineering in anti-microsporidian research and reagent construction.

Knockout of BmIDH inhibits microsporidian proliferation, further confirming the importance of BmIDH to microsporidia. The utilization of host metabolic pathways is a necessary parasitic behavior of microsporidia, and while this reflects the success of microsporidian parasitism, excessive dependence on host energy supply may also constitute a vulnerability. Correspondingly, the importance of BmIDH to microsporidia gives it potential as a molecular target for anti-microsporidian interventions. Studies on glucose uptake in host cells further revealed that BmIDH overexpression enhances cellular glucose absorption. Treatment with the glucose transporter inhibitor BAY-876 significantly impairs cellular glucose uptake capacity, leading to a substantial reduction in intracellular ATP synthesis and subsequent inhibition of microsporidian proliferation. This suggests that BAY-876 also holds potential as an anti-microsporidian drug.

V. CONCLUSIONS

BmIDH localizes to the cytoplasm and exhibits colocalization with cellular mitochondria. BmIDH enhances cellular metabolic capacity by accelerating the tricarboxylic acid (TCA) cycle process, improving cellular ATP synthesis ability, and promoting glucose uptake. Quantitative detection of NbSSU showed that BmIDH expression promotes microsporidian proliferation, and microsporidian proliferation is impaired after CRISPR/Cas9-mediated knockout of BmIDH, indicating that BmIDH plays a critical role in the intracellular parasitism of microsporidia. Treatment with the GLUT-specific inhibitor BAY-876 showed an inhibitory effect on microsporidian proliferation.Functional analysis of key host response genes can provide potential molecular targets and drug targets for anti-microsporidian research.

Acknowledgments: This work was supported by the Sichuan Science and Technology Program 2023NSFSC1149）, Science Foundation of Sichuan University of Science & Engineering (2021RC04)

Compliance with ethical standards

Conflict of interest

Authors declare that they have no potential conflicts of interests.

Ethical approval

This article does not contain any experiments with human participants or animals (except invertebrate's cell lines, which are exempt from ethical concerns) performed by any of the authors.

REFERENCES

[1]. Canning EU. CHAPTER 4–Microsporidia. parasitic protozoa[M]. 1993.
[2]. Xu Y, Weiss LM. The microsporidian polar tube: a highly specialised invasion organelle[J]. Int J Parasitol, 2005, 35(9): 941-953.
[3]. Capella-Gutierrez S, Marcet-Houben M, Gabaldon T. Phylogenomics supports microsporidia as the earliest diverging clade of sequenced fungi[J]. BMC Biol, 2012, 10: 47.
[4]. Arisue N, Sanchez LB, Weiss LM, Muller M, Hashimoto T. Mitochondrial-type hsp70 genes of the amitochondriate protists, Giardia intestinalis, Entamoeba histolytica and two microsporidians[J]. Parasitol Int, 2002, 51(1): 9-16.
[5]. Thomarat F, Vivares CP, Gouy M. Phylogenetic analysis of the complete genome sequence of Encephalitozoon cuniculi supports the fungal origin of microsporidia and reveals a high frequency of fast-evolving genes[J]. J Mol Evol, 2004, 59(6): 780-791.
[6]. Higes M, Martin-Hernandez R, Botias C, Bailon EG, Gonzalez-Porto AV, Barrios L, Del Nozal MJ, Bernal JL, Jimenez JJ, Palencia PG, Meana A. How natural infection by Nosema ceranae causes honeybee colony collapse[J]. Environ Microbiol, 2008, 10(10): 2659-2669.
[7]. Antunez K, Martin-Hernandez R, Prieto L, Meana A, Zunino P, Higes M. Immune suppression in the honey bee (Apis mellifera) following infection by Nosema ceranae (Microsporidia)[J]. Environ Microbiol, 2009, 11(9): 2284-2290.
[8]. Pan G, Xu J, Li T, Xia Q, Liu SL, Zhang G, Li S, Li C, Liu H, Yang L, Liu T, Zhang X, Wu Z, Fan W, Dang X, Xiang H, Tao M, Li Y, Hu J, Li Z, Lin L, Luo J, Geng L, Wang L, Long M, Wan Y, He N, Zhang Z, Lu C, Keeling PJ, Wang J, Xiang Z, Zhou Z. Comparative genomics of parasitic silkworm microsporidia reveal an association between genome expansion and host adaptation[J]. BMC Genomics, 2013, 14: 186.
[9]. Vávra J. Structure of the Microsporidia. Biology of the microsporidia[M]. US: Springer US.
[10]. Keohane EM, Weiss LM. Chapter 6: The Structure, function, and composition of the microsporidian polar tube[M]. 1999.
[11]. Williams BA, Dolgikh VV, Sokolova YY. Microsporidian biochemistry and physiology. Microsporidia: pathogens of opportunity[J]. 2014.
[12]. Akiyoshi DE, Morrison HG, Lei S, Feng X, Zhang Q, Corradi N, Mayanja H, Tumwine JK, Keeling PJ, Weiss LM, Tzipori S. Genomic survey of the non-cultivatable opportunistic human pathogen, Enterocytozoon bieneusi[J]. PLoS Pathog, 2009, 5(1): e1000261.
[13]. Cornman RS, Chen YP, Schatz MC, Street C, Zhao Y, Desany B, Egholm M, Hutchison S, Pettis JS, Lipkin WI, Evans JD. Genomic analyses of the microsporidian Nosema ceranae, an emergent pathogen of honey bees[J]. PLoS Pathog, 2009, 5(6): e1000466.
[14]. Corradi N, Haag KL, Pombert JF, Ebert D, Keeling PJ. Draft genome sequence of the Daphnia pathogen Octosporea bayeri: insights into the gene content of a large microsporidian genome and a model for host-parasite interactions[J]. Genome Biol, 2009, 10(10): R106.
[15]. Corradi N, Pombert JF, Farinelli L, Didier ES, Keeling PJ. The complete sequence of the smallest known nuclear genome from the microsporidian Encephalitozoon intestinalis[J]. Nat Commun, 2010, 1: 77.
[16]. Heinz E, Lithgow T. Back to basics: a revealing secondary reduction of the mitochondrial protein import pathway in diverse intracellular parasites[J]. Biochim Biophys Acta, 2013, 1833(2): 295-303.
[17]. Lin L, Pan G, Li T, Dang X, Deng Y, Ma C, Chen J, Luo J, Zhou Z. The protein import pore Tom40 in the microsporidian Nosema bombycis[J]. J Eukaryot Microbiol, 2012, 59(3): 251-257.
[18]. Yu SY, Liu ZG, Jia Q, Chen LC, Lu Y. Research progress on relationship between glucose transporter 1 and tumor energy metabolism[J]. Chinese Pharmacological Bulletin, 2016.
[19]. Roberts DJ, Miyamoto S. Hexokinase II integrates energy metabolism and cellular protection: Akting on mitochondria and TORCing to autophagy[J]. Cell Death Differ, 2015, 22(2): 364.
[20]. Diers AR, Broniowska KA, Chang CF, Hogg N. Pyruvate fuels mitochondrial respiration and proliferation of breast cancer cells: effect of monocarboxylate transporter inhibition[J]. Biochem J, 2012, 444(3): 561-571.
[21]. Kurze C, Dosselli R, Grassl J, Le Conte Y, Kryger P, Baer B, Moritz RF. Differential proteomics reveals novel insights into Nosema-honey bee interactions[J]. Insect Biochem Mol Biol, 2016, 79: 42-49.
[22]. He X, Fu Z, Li M, Liu H, Cai S, Man N, Lu X. Nosema bombycis (Microsporidia) suppresses apoptosis in BmN cells (Bombyx mori)[J]. Acta Biochim Biophys Sin (Shanghai), 2015, 47(9): 696-702.
[23]. Jarkass HTE, Reinke AW. The ins and outs of host-microsporidia interactions during invasion, proliferation and exit[J]. Cell Microbiol, 2020, 22(11): e13247.
[24]. Dean P, Hirt RP, Embley TM. Microsporidia: Why make nucleotides if you can steal them?[J]. PLoS Pathog, 2016, 12(11): e1005870.